International Journal of Modern Physics B
Vol. 31, No. 10 (2017) 1742012 (13 pages)

DOI: 10.1142/S0217979217420127

Impact decimation using alignment of granular spheres

Mukesh Tiwari

*Group in Computational Science and High Performance Computing,
Dhirubhai Ambani Institute of Information and Communication Technology (DA-IICT),
Gandhinagar, Gujarat 382421, India
mukesh_tiwari@daiict.ac.in*

T. R. Krishna Mohan

*CSIR Fourth Paradigm Institute
(formerly CSIR Center for Mathematial Modelling and Computer Simulation (C-MMACS)),
NAL WTC Road, Bangalore 560037, India
kmohan@cmmacs.ernet.in*

Surajit Sen

*Department of Physics, State University of New York Buffalo,
New York 14260-1500, USA
sen@buffalo.edu*

Received 26 October 2016
Revised 23 December 2016
Published 17 March 2017

Solitary waves in alignment of elastic beads have been an important area of study. An important and rich area has been the behavior of solitary waves at a boundary, where features such as localization, anomalous behavior in scattering and transmission, quasiequilibrium phase, etc. are being studied. An application area of significance is the design of artificial granular alignments for shock decimation and dispersion. In this review article, we first present a summary and background of these unique features, and some designs in 1D which exploit these features. We further discuss some extensions to higher dimensional systems and their impact decimation ability.

Keywords: Granular media; solitary wave disintegration; impact decimation; decorated granular arrangement.

PACS numbers: 45.70.-n, 83.80.Fg, 46.40.Cd

1. Introduction

The study of solitary waves in arrangement of granular chains has a long history. Starting with the pioneering work of Nesterenko[1,2] who showed the existence of solitary waves in a chain of uncompressed spheres, significant advance has been made in the fundamental understanding of these waves. The important aspect about such systems is that, within certain limits, they can be modeled as point mass interacting through the nonlinear Hertz interaction[3] $F = k\delta^{3/2}$, where δ is the overlap parameter and k is a spring constant which depends on the material parameters. Nesterenko showed that within the long wavelength approximation, such systems have solitary wave solutions, in which the speed of the traveling wave depends on its amplitude and the wave has a small spatial extent (roughly around five grains). The properties of these solitary waves have since been studied in great detail through computer simulations, analytical methods (see Refs. 4, 5 and references therein), and have also been observed experimentally.[6,7] The structure of these solitary waves depends on both the initial conditions such as nature of loading and precompression[8,9] which lead to its generation, and the geometric and material properties (mass, radius, density ρ, Young's modulus Y, Poisson ratio ν) of the granular medium. The dynamics of ordered granular media has since attracted a lot of attention which have been geared towards the fundamental understanding of energy propagation in such discrete systems. This has also been instrumental in recognizing their abilities towards many potential engineering applications (see Ref. 10 and references therein). The primary reason being that these properties are highly tunable. A solitary wave shows unique properties when it crosses an interface to another granular medium composed of grains with different mass, size and elastic properties, which can be utilized particularly in the creation of impaction dispersion and mitigation devices.[11–14] It is important to point out that restitution losses and other forms of dissipation can also result in weakening of the pulses. Our focus in this article is, however, only on the weakening that results because of the dynamics in the presence of interfaces. In this paper, we discuss these properties and some relevant geometries that have been suggested which effectively exploit them and are useful in the design of efficient shock dispersion and absorption systems.

2. 1D Alignment for Impact Decimation

One-dimensional (1D) systems are important test bed for theoretical and experimental studies. Not only are they useful in developing insight and intuition, they also turn out to be the simplest building block for higher dimensional systems. In 1D, the different geometries for impact decimation can be broadly classified into two types, the tapered chain and the composite chain arrangement.

2.1. *Tapered chain*

The tapered chain or the simple tapered chain (STC) arrangement was proposed by Sen *et al.*,[15,16] and consists of an alignment of elastic spheres, in which, the spheres progressively shrink in radius according to a tapering factor q ($r[i] = (1 - q)r[i-1]$) along the length of the chain [shown in Fig. 1 (left)], and has also been realized experimentally.[17] Typical energy propagation in an elastic tapered chain arrangement is shown in Fig. 1. As the pulse moves through the chain its

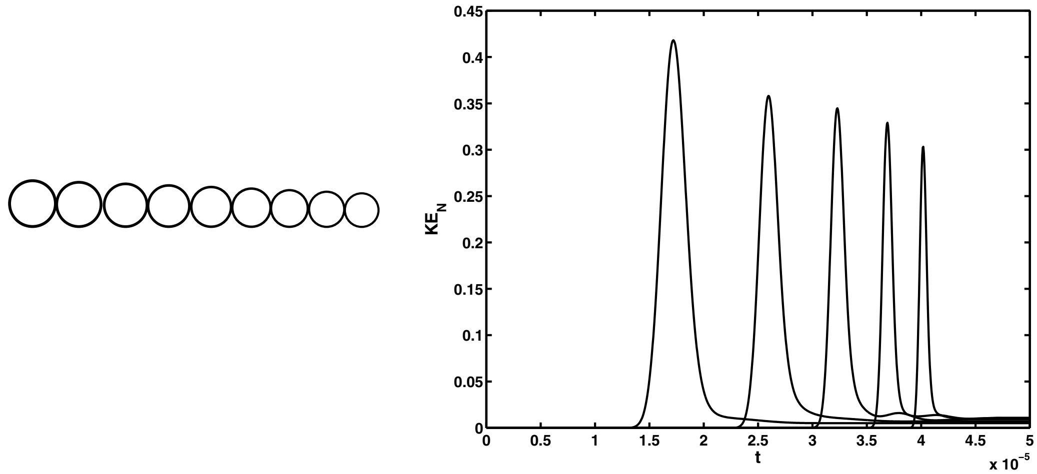

Fig. 1. (Left) Schematic of a tapered chain. (Right) Typical kinetic energy propagation in a tapered chain with free ends.

amplitude attenuates, as a result of the breaking of translational symmetry due to the inertial mismatch between adjacent grains. The pulse as it moves to the lighter grain accelerates and in the process leaves behind energy in the heavier grain. The mechanics can be understood at a coarser level by ignoring the nonlinear interaction and considering a typical collision of two point masses m_1 and m_2. If the mass m_2 is initially at rest, then the fraction of kinetic energy that remains with mass m_1 after collision would be given by $KE_N = \left(\frac{1-\epsilon}{1+\epsilon}\right)^2$ $(\epsilon = m_1/m_2)$. For unequal masses $(\epsilon \neq 1)$, only a part of the energy is transmitted and is controlled by ϵ, which in turn is controlled by the density and radius of the two spheres. The tapered chain introduces inhomogeneity in mass in the chain through a variation in radius of each sphere. Using hard sphere approximation and energy and momentum conservation, it has been shown that the fraction of energy reaching the other end of the chain is given by[15,17]

$$KE_N = \left[\frac{4(1-q)^3}{1+(1-q)^3}\right]^{N-1} . \tag{1}$$

The amount of tapering q and the number of grains N are the significant parameters that determine the shock absorption ability of tapered chains. It has been shown, for example, that a tapered chain with 20 spheres that are made from strong, light-mass material can absorb 80–90% of the incident energy.[18] It is also evident that increasing the mass mismatch between adjacent grains further improves the shock absorption ability of such chains. A configuration which takes advantage of this feature is the decorated tapered chain (DTC).[19] In a decorated chain, interstitial spheres, the sizes of which are a fraction of the smallest sphere in a simple tapered are inserted at each contact. The frequent large mass mismatch improves the impact decimation of the tapered chain by providing better momentum traps. The hard sphere approximation results for the decorated chain show qualitative agreement with the results obtained from numerical simulations, and the long wavelength approximation approach is difficult to implement due to the spatial variation of the wave structure. Lindenberg *et al.* have developed a theoretical approach for such systems called the binary collision approximation (BCA)[20–22] and used it to study the different forms of tapered chain such as backward and forward linearly and exponentially tapered chain, decorated and randomly decorated chains. The BCA approximates the pulse extent at any instant of time to two particles and then solves the resulting equation of motion. Their analysis while overpredicting the pulse amplitude captures the pulse speed, its residence time and decay rate remarkably well.

2.2. *Composite*

A composite chain is different from a tapered chain, in that, it is constructed by assembling different sections. The properties of the particles in each section is kept the same. The properties of different sections of the chain are varied by having particles of different material or radius. An important feature of the solitary wave is that when it moves from a region of heavy granules to a region of light granules, the pulse is completely transmitted and it also disintegrates into well-separated pulses or solitary wave trains (SWT) with decreasing amplitude. However, if the pulse is incident from the lighter side, then this feature is not observed and there exists a reflected and a transmitted component.[14,23] Disintegration is observed in the backscattered or reflected component. The same behavior is present in chains made with materials with different elastic moduli. In a chain composed of steel ($Y = 193$ GPa) and PTFE ($Y = 1.46$ GPa) sections, it was observed that the amplitude of the reflected component is $\sim 75\%$ of the amplitude of the incident wave when the wave is incident from the PTFE section.[13] The difference in backscattering depending on the presence of lighter or heavier impurity can be used for nondestructive identification of impurities in a granular medium.[11,24] This feature also provides another effective shock protection mechanism called the granular container first proposed by Hong.[25] It was shown that pulses could be confined temporarily in a chain which consists of a light section sandwiched on either side with sections made up of heavier material. A granular container breaks a pulse incident from the heavy side into weak pulses and confines them in the lighter section of the chain. Energy is slowly leaked every time it reaches the boundary of the lighter section. Impulse confinement and weak release of energy have also been observed experimentally in a composite granular system where the lighter section made of material with orders of magnitude smaller elastic moduli[26] serves as the container. The nature of transmission from the two interfaces of the container is also significantly different. The transmission at the lower end of the container is elastic, whereas the transmission at the top end is seen to be delayed in time, where the pulse freezes before moving to the heavier section resulting in a phenomenon termed as gap opening.[26,27] The relationship between

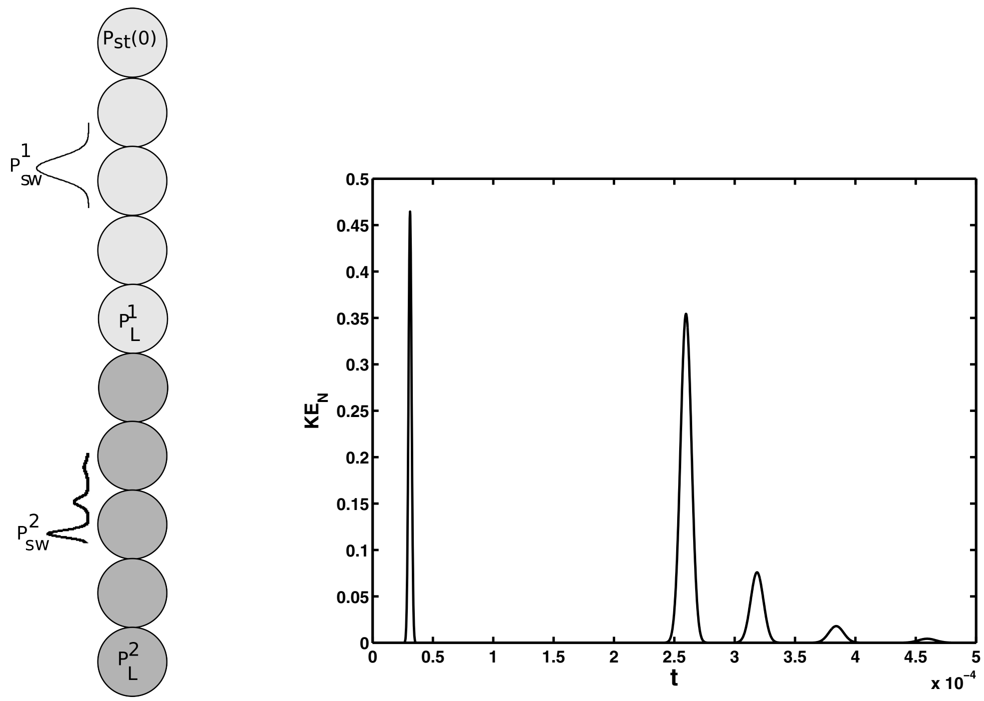

Fig. 2. (Left) Composite granular protector. (Right) Kinetic energy propagation in a composite chain arrangement with the top section made of steel spheres with density 8000 kg/m^3 and the lower section made of Teflon with density 2170 kg/m^3.

the amplitudes of the pulses in the SWT has been observed to be exponentially decreasing.[9] Job *et al.*[8] studied the wave trains under impact loading when a massive striker hits a chain of monosized spheres, and when the chain has two sections with different radii. To get an estimate of the amplitude of the pulses in the SWT, they used a quasiparticle approach. In the quasiparticle approach, the solitary wave is approximated by a single particle with an effective mass, and has the momentum and energy of the solitary wave. More recently, the quasiparticle approach has been successfully used to predict the amplitudes of the transmitted solitary waves generated when an incident solitary-wave front, parallel to the interface, moves from a denser to a lighter section in a granular hexagonal lattice by Tichler *et al.*[28] Under the quasiparticle approximation, let us try to understand the basic idea behind impact decimation by a composite chain. In the quasiparticle assumption, the effective mass of the solitary wave is given by $m_{\text{eff}} = \Omega m$, where Ω is approximately 1.4 and m is the mass of the spheres in the chain. Let us consider a chain made of two sections in which the mass of spheres in the top section is m_1 and mass of spheres in the bottom section is m_2 ($m_1 > m_2$). We also assume that the impulse is given to the top sphere in the first section. As shown in the right in Fig. 2 the energy travels as a single pulse in the top section and degenerates into well-separated pulses in the second section. If we further assume that the length of each section is such that we get fully developed and clearly separated pulses, then the peak value of momentum of the leading pulse in the second section can be calculated via the discrete sequence of momentum transfer events [shown in Fig. 2(left)]). The first event here is taken as a two body collision between the striker and the solitary wave in the top section treated as a quasiparticle. In the next event momentum transfer occurs between the solitary wave and the last particle in the top section, and finally, the momentum transfer resulting from the collision of the last sphere in the top section with the leading pulse of the solitary wave in the second section. Mathematically, the ratio of the peak amplitude of the momentum of the leading pulse in the second section to the initial striker momentum can be written as

$$\frac{p_{sw}^2}{p_{st}(0)} = \left(\frac{p_{sw}^2}{p_L^1}\right)\left(\frac{p_L^1}{p_{sw}^1}\right)\left(\frac{p_{sw}^1}{p_{st}(0)}\right),$$
$$\frac{p_{sw}^2}{p_{st}(0)} = \left(\frac{2}{1+\Omega}\right)\left(\frac{2\Omega}{\Omega+\epsilon}\right)\left(\frac{2\Omega}{\Omega+1}\right). \tag{2}$$

For the parameter values used in Fig. 2, the ratio of the peak amplitude of the energy of the solitary wave in the two sections is 0.78, which is close to 0.76, the value obtained from numerical simulation. It is important to note that this method does not predict the correct value if the impact is from the lighter section. Apart from the design aspects[29–31] fundamental questions related to the steady state behavior or quasi-equilibrium[32] are also being explored.

3. Impact Decimation using granular alignments in 2D and 3D

A practical impulse protector must be three-dimensional (3D). Impact decimation systems in higher dimensions can also be realized by random packing of particles.[33–41] Their impact absorption ability is determined through the drag force experienced by a projectile hitting a granular bed. This is done via analysis based on penetration depth, morphology of the crater and the force chain distributions. The nature of the packing of the particles as evident in the porosity, fabric and coordination number plays an important role in such systems. Energy propagation occurs through the force chain structures, which in many situations are very complex. Another method is by constructing artificial protectors which manipulate and take advantage of the rich behavior of 1D granular arrangements. The simplest way to realize this is by enclosing the granular chains in a matrix and creating higher dimensional structures through parallel arrangement of many of such matrix.[30,42] More recently, a forward tapered chain, decorated with granules that are not aligned along the central axis, has been suggested.[43] Numerical studies have shown that this arrangement provides 20% improvement in impact decimation as compared to the simple tapered chain. Impact studies on purely two-dimensional (2D) system was started by Shukla *et al.* who in a series of experimental and numerical work have explored the wave propagation and dynamic load transfer path in granular arrangements.[44–49] Nishida *et al.* have experimentally and numerically studied projectile impact and wave propagation in 2D granular arrangement.[50–52] The force experienced by the base plate has been used as a measure of the impact absorption, and it was observed that by increasing the number of layers or introducing layers made of dissimilar materials leads to the reduction of the force. Much of these are however focused on rectangular and hexagonal arrangement of granular particles. A square or rectangular arrangement of monosized spheres supports solitary waves similar to 1D packing[53,54] and could be useful in directional propagation of waves. In a hexagonal packing, energy spreads over more and more grains as it propagates[55] and therefore, hexagonal arrangement would be a suitable configuration for impact dispersion. A square packing can also be used for impact dispersion by introduction of interstitial atoms.[56–60] Leonard *et al.* have recently proposed and analyzed a structured network in which the initial section divides into symmetric sections.[61,62] The leading pulse amplitude propagating in the system showed exponential decrease. Studies on wave propagation in 3D geometries have also gained momentum recently.[63–65]

3.1. *Decorated granular arrangement for impact decimation*

Taking the point of view that both the mass and material mismatches are important considerations for impact decimation, we can have an arrangement[66] as shown in Fig. 3. The system here consists of a square arrangement of granular particles in a block type arrangement. The spheres in each block have the same mass and material properties. The radius of the spheres in each block is, however, twice that of the spheres in the block immediately below it. An impact at the top of the arrangement propagates through the vertical chains of spheres in the top block. The nature of energy dispersion can be understood from the sphere arrangement at the interface. Since the larger sphere is placed on top of two smaller spheres, the energy reaching it gets distributed in the two smaller spheres. This energy then travels both sideways and downward along the chain of spheres in contact with it. We assume that the length of each block is large enough to lead to the generation of solitary wave pulses. This process then gets repeated at each interface. At each interface, the mass mismatch leads to disintegration of the pulse, and the sphere arrangement leads to the dispersion of energy into more number of spheres. Within the hard sphere approximation and considering only the system of a single large sphere supported by two smaller spheres [see enlarged view of the interface in Fig. 3 (top)], the energy along different propagation directions is given by

$$\frac{E_d}{E_0} = \frac{4\epsilon\cos^4\theta}{(\epsilon + 2\cos^2\theta)^2}\,, \tag{3}$$

$$\frac{E_s}{E_0} = \frac{\epsilon\sin^2 2\theta}{(\epsilon + 2\cos^2\theta)^2}\,, \tag{4}$$

$$\frac{E_r}{E_0} = \left(\frac{\epsilon - 2\cos^2\theta}{\epsilon - 2\cos^2\theta}\right)^2\,. \tag{5}$$

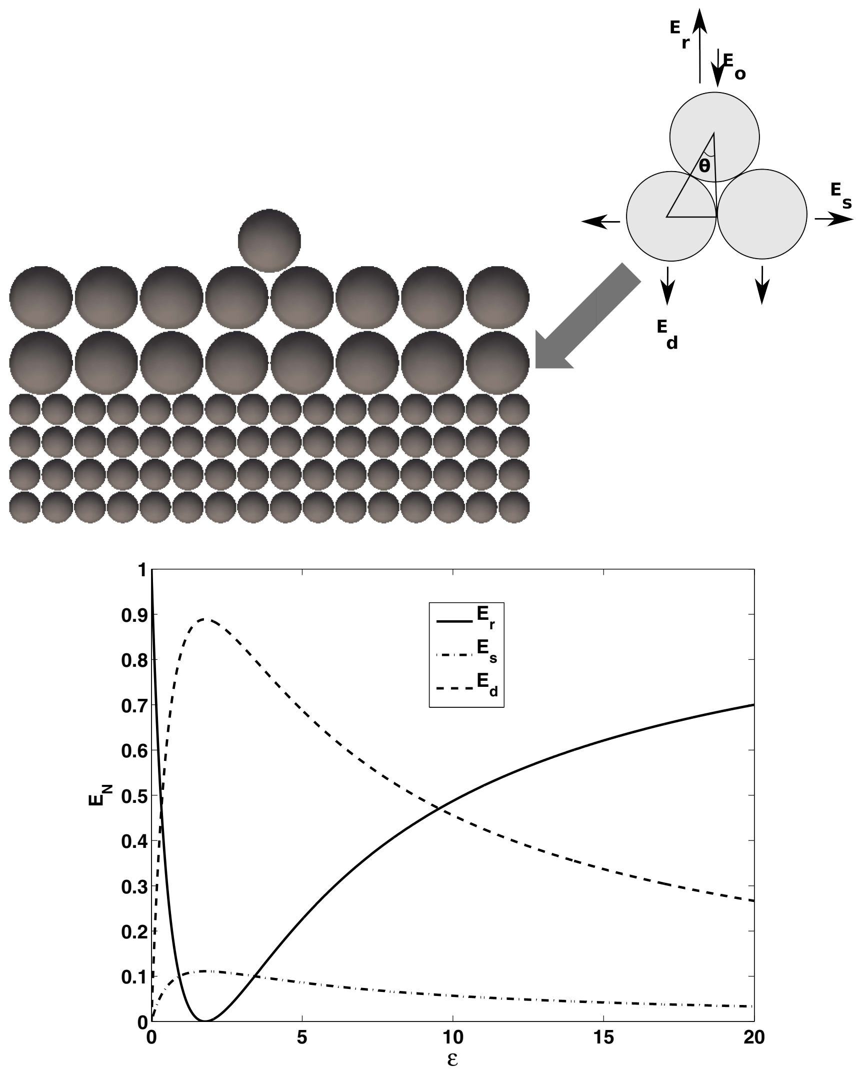

Fig. 3. (Top) Schematic of 2D decorated layers, inset shows the enlarged view of the sphere arrangement at the interface. (Bottom) Distribution of energy along different propagation directions for the three sphere arrangement shown in the inset.

E_0 is the initial instantaneous energy of the larger sphere. E_d and E_s are the energies propagating downward and sideways through one of the smaller spheres, while E_r is the energy retained by the larger sphere. The angle θ appears because of the geometry and equals $\cos^{-1}(2\sqrt{2}/3)$. As shown in Fig. 3 the energy transmitted in the first collision can be reduced by taking $\epsilon \ll 1$ or $\epsilon \gg 1$. The former condition corresponds to reflection of the larger sphere, while in the latter, it continues to move in its original direction. The second region would therefore provide more flexibility in the choice of materials and design. If the spheres in different blocks are made of the same material, then the mass difference is only due to difference in size, ϵ equals 8, and E_d is around 26% while E_s is around 3%. Increasing the values

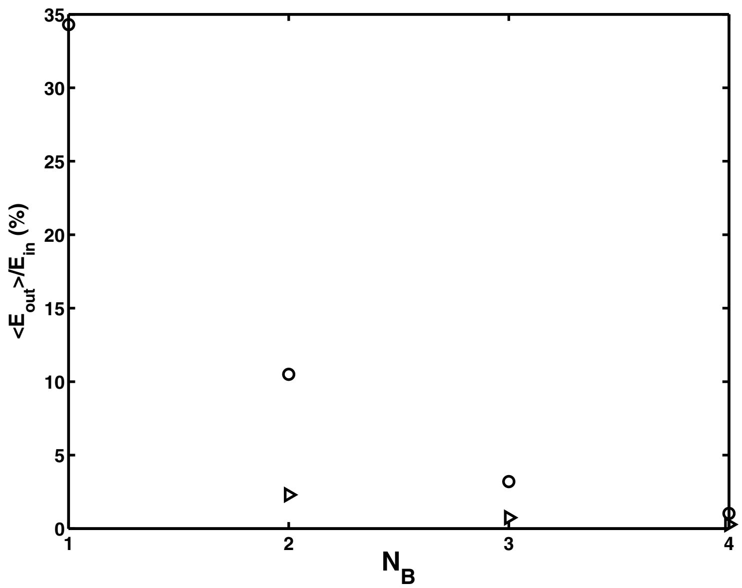

Fig. 4. Comparison of the average output kinetic energy for $1-4$ block system with all blocks made of steel (o) and alternating blocks and steel and teflon particle ▹.

of the mass ratio would further enhance the disintegration of the pulse. This can be accomplished by introducing softer materials in the second block. Softer particles also lead to slowing of the waves. We can therefore envision a construction in which there are two types of materials, hard and soft with different density. The impulse disintegrates and slows down in the softer section, and when it arrives at the soft-hard interface, it is rapidly carried away by the block with harder spheres. Figure 4 shows the fraction of average kinetic energy in the bottommost layer for the two cases with the number of blocks varying from 1 to 4. The lighter material used here is teflon and the heavier is steel. While both cases show strong impact decimation ability, it is further enhanced as expected in the one with lighter material.

This can also be understood from Fig. 3. The mass ratio for the steel–teflon interface is approximately 30, while it is approximately 2 at the teflon–steel interface. For the arrangement with spheres made from the same material, it is the same at all the interface and equals 8. The larger mass mismatch at the top interface leads to less energy being transmitted at the first collision. At the second interface, the larger value for steel–steel interface does not have much of an impact since the pulses are already very weak when they approach this interface. From Eq. (5), for the material considered here, the pulses always move from denser to lighter medium and hence, no backscattering is observed. For block lengths such that solitary waves are formed, this also allows for the application of the quasiparticle theory discussed in the earlier section, and its predictions are in close agreement with the values obtained from numerical simulations. For block lengths which are smaller, the values are slightly lower and the quasiparticle theory shows only qualitative agreement. For such situations, the BCA should be a better approach.

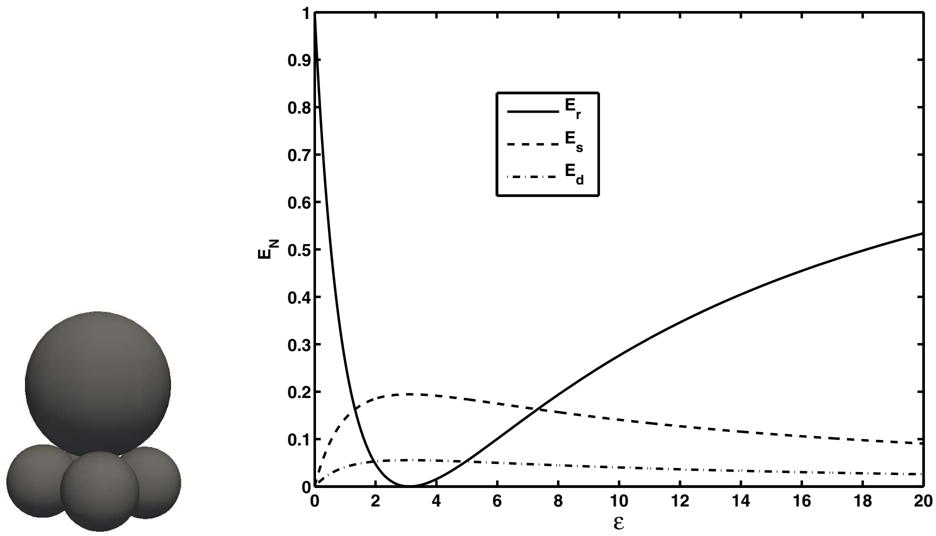

Fig. 5. (Left) Schematic of the sphere arrangement at the interface for a 3D decorated granular protector. (Right) Distribution of energy along different propagation directions.

3.2. *Impact decimation with decorated layers in 3D*

The decorated packing in 2D can be easily extended to 3D. It has been suggested that in a cubic packing, waves should propagate similar to the 1D chains.[2] We can therefore have blocks with cubic packing of spheres, and a similar decorated arrangement at the interface, such that the radius of the sphere at the interface is twice that of the spheres below it.[67] The difference is that the larger sphere is in contact with four smaller spheres at the interface, which leads to enhanced dispersion ability for the 3D arrangement. For the sphere arrangement at the interface as shown in Fig. 5 (left), the energy propagating along different directions through each of the spheres is given by

$$\frac{E_d}{E_0} = \frac{4\epsilon\cos^4\theta}{(\epsilon + 4\cos^2\theta)^2}\,, \tag{6}$$

$$\frac{E_s}{E_0} = \frac{\epsilon\sin^2 2\theta}{(\epsilon + 4\cos^2\theta)^2}\,, \tag{7}$$

$$\frac{E_r}{E_0} = \left(\frac{\epsilon - 4\cos^2\theta}{\epsilon - 4\cos^2\theta}\right)^2\,, \tag{8}$$

which is similar to Eqs. (3)–(5) except for the factor of 4 instead of 2 before the cosine term in the denominator and the value of angle θ which equals $\cos^{-1}(\sqrt{7}/3)$. As is evident from Fig. 5 (right), the fraction of energy being transmitted to the smaller spheres is significantly smaller than in 2D decorated sphere arrangement. The distribution and propagation of energy for the complete setup with composite packing (steel–teflon–steel) is shown in Fig. 6. The spheres in the top block are

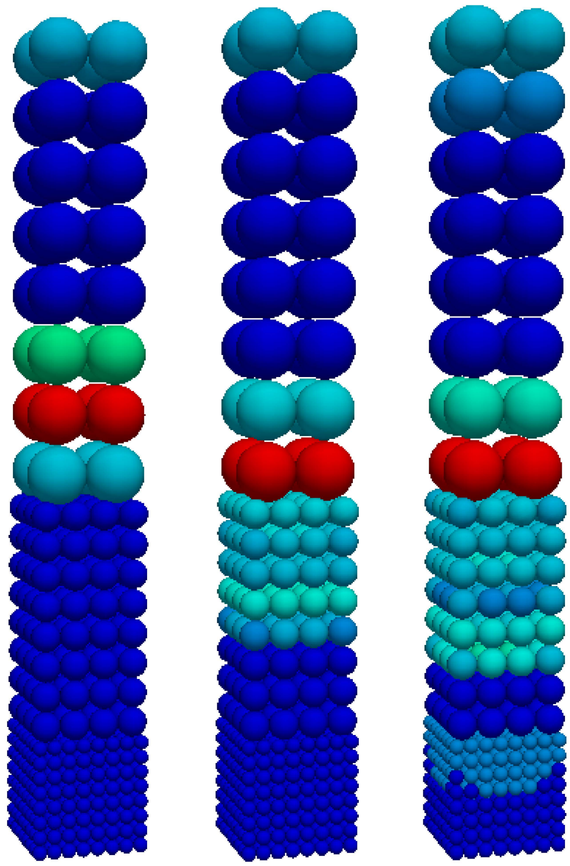

Fig. 6. (Color online) Vertical propagation of energy in a 3D composite granular protector with three blocks at different time instants. The spheres are colored with the normalized kinetic energy for that particular time instant.

excited in such a way that energy propagates as a single solitary wave through four vertical chains in the top section. The primary features of wave propagation are the same as in the 2D decorated arrangement. The solitary waves split into smaller pulses at the top interface, slowly leaks into the teflon block, and finally, is carried away rapidly by the last block. However, we also observe backscattering at the second interface which was not present in the 2D studies. With the same material parameters but because of the geometry, we have $\epsilon < 4\cos^2\theta$ in Eq. (8). The 3D setup here shows superior impact decimation properties than its 2D counterpart, both because of enhanced dispersion and backscattering at the second interface.

4. Conclusions

In this article, we have presented a review of some granular alignments that have the potential to mitigate shocks substantially. Conceptually, it involves breaking the impulse into smaller pulses and then spreading them out in space to mitigate their impact. In order to achieve this, the unique features exhibited by solitary waves in system of granular particles at interfaces are exploited. Based on the experience gained through the study of 1D systems, we have discussed in detail one simple geometry which maximizes these advantages in higher dimensions. The presentation here has considered wave propagation in uncompressed elastic spheres. However, in the design of realistic systems, effects of precompression, dissipation, confining conditions will also have a pronounced effect. Current research aims also include developing a comprehensive understanding of these effects on wave propagation.[68–72]

References

1. V. F. Nesterenko, *J. Appl. Mech.Tech. Phys.* **24**, 733 (1983).
2. V. F. Nesterenko, *Dynamics of Heterogeneous Materials* (Springer, New York, 2001).
3. H. Hertz, *J. Reine Angew. Math.* **92**, 156 (1881).
4. S. Sen *et al.*, *Phys. Rept.* **462**, 21 (2008).
5. P. G. Kevrekidis, *IMA J. Appl. Math.* **76**, 389 (2011).
6. A. N. Lazaridi and V. F. Nesterenko, *J. Appl. Mech. Tech. Phys.* **26**, 405 (1985).
7. C. Coste, E. Falcon and S. Fauve, *Phys. Rev. E* **56**, 6104 (1997).
8. S. Job *et al.*, *Gran. Matter* **10**, 13 (2007).
9. A. Sokolow, E. G. Bittle and S. Sen, *Eur. Phys. Lett.* **77**, 24002 (2007).
10. M. A. Porter, P. G. Kevrekidis and C. Daraio, *Phys. Today* **68**, 44 (2015).
11. J. Hong and A. Xu, *Appl. Phys. Lett.* **81**, 4868 (2002).
12. S. Job *et al.*, *Phys. Rev. Lett.* **94**, 178002 (2005).
13. V. F. Nesterenko *et al.*, *Phys. Rev. Lett.* **95**, 158702 (2005).
14. L. Vergara, *Phys. Rev. Lett.* **95**, 108002 (2005).
15. S. Sen, M. Manciu and F. S. Manciu, *Physica A* **299**, 551 (2001).
16. R. Doney and S. Sen, *Phys. Rev. E* **72**, 041304 (2005).
17. M. Nakagawa *et al.*, *Gran. Matter* **4**, 167 (2003).
18. A. Sokolow *et al.*, *Appl. Phys. Lett.* **87**, 254104 (2005).
19. R. Doney and S. Sen, *Phys. Rev. Lett.* **97**, 155502 (2006).
20. U. Harbola *et al.*, *Phys. Rev. E* **80**, 031303 (2009).
21. U. Harbola *et al.*, *Phys. Rev. E* **80**, 051302 (2009).
22. U. Harbola *et al.*, *Phys. Rev. E* **82**, 011306 (2010).
23. V. F. Nesterenko, A. N. Lazaridi and E. B. Sibiryakov, *J. Appl. Mech. Tech. Phys.* **36**, 166 (1995).
24. S. Sen, M. Manciu and J. D. Wright, *Phys. Rev. E* **57**, 2386 (1998).
25. J. Hong, *Phys. Rev. Lett.* **94**, 108001 (2005).
26. C. Daraio *et al.*, *J. Phys. IV France* **134**, 473 (2006).
27. L. Vergara, *Phys. Rev. E* **73**, 066623 (2006).
28. A. M. Tichler *et al.*, *Phys. Rev. Lett.* **111**, 048001 (2013).
29. F. Fraternali, M. A. Porter and C. Daraio, *Mech. Adv. Mater.* **17**, 1 (2010).
30. A. Breindel, D. Sun and S. Sen, *Appl. Phys. Lett.* **99**, 063510 (2011).
31. M. A. Przedborski, T. A. Harroun and S. Sen, *Appl. Phys. Lett.* **107**, 244105 (2015).
32. M. A. Przedborski, T. A. Harroun and S. Sen, *Phys. Rev. E* 9**1**, 042207 (2015).
33. J. Uehara *et al.*, *Phys. Rev. Lett.* **90**, 194301 (2003).
34. H. Katsuragi and D. J. Durian, *Nat. Phys.* **3**, 420 (2007).
35. D. I. Goldman and P. Umbanhowar, *Phys. Rev. E* **77**, 021308 (2008).
36. M. A. Ambroso, R. D. Kamien and D. J. Durian, *Phys. Rev. E* **72**, 041305 (2005).
37. M. P. Ciamarra *et al.*, *Phys. Rev. Lett.* **92**, 194301 (2004).
38. A. H. Clark, L. Kondic and R. P. Behringer, *Phys. Rev. Lett.* **109**, 238302 (2012).

39. F. Bourrier, F. Nicot and F. Darve, *Gran. Matter* **10**, 415 (2008).
40. M. Tiwari, T. R. K. Mohan and S. Sen, *Phys. Rev. E* **90**, 062202 (2014).
41. H. Katsuragi, *Physics of Soft Impact and Cratering* (Springer, Tokyo, 2016).
42. R. L. Doney and S. Sen, Shock mitigation for blast protection using Hertzian tapered chains, in *Proc. 22nd Int. Symp. Ballistics*, Vancouver, BC, 14–18 November (2005), p. 14.
43. L. P. Machado, A. Rosas and K. Lindenberg, *Eur. Phys. J. E* **37**, 119 (2014).
44. H. P. Rossmanith and A. Shukla, *Acta Mech.* **42**, 211 (1982).
45. A. Shukla and C. Damania, *Exp. Mech.* **27**, 268 (1987).
46. M. H. Sadd, A. Shukla and H. Mei, Computational and experimental modeling of wave propagation in granular materials, in *Proc. 4th Int. Conf. Computational Methods and Experimental Measurements*, Capri, Italy (1989), pp. 325–334.
47. A. Shukla, M. H. Sadd and H. Mei, *Exp. Mech.* **30**, 377 (1991).
48. M. H. Sadd, Q. Tai and A. Shukla, *Int. J. Nonlinear Mech.* **28**, 251 (1993).
49. Y. Zhu, A. Shukla and M. Sadd, *J. Mech. Phys. Solids* **44**, 1283 (1996).
50. M. Nishida *et al.*, Discrete element simulation in projectile impacts on granular materials, in *Proc. 23rd Int. Symp. Shock Waves* (2001), pp. 655–661.
51. K. Tanaka *et al.*, *Powder Technol.* **124**, 160 (2002).
52. M. Nishida and Y. Tanaka, *Gran. Matter* **12**, 357 (2010).
53. M. S. Abd-Elhady *et al.*, *Adv. Powder Technol.* **21**, 150 (2010).
54. A. Leonard, F. Fraternali and C. Daraio, *Exp. Mech.* **57**, 327 (2013).
55. A. Leonard *et al.*, *Gran. Matter* **16**, 531 (2014).
56. I. Szelengowicz, P. G. Kevrekidis and C. Daraio, *Phys. Rev. E* **86**, 061306 (2012).
57. A. Leonard and C. Daraio, *Phys. Rev. Lett.* **108**, 21430 (2012).
58. A. Leonard *et al.*, *Phys. Rev. E* **86**, 031305 (2012).
59. A. P. Awasthi *et al.*, *Mech. Mater.* **54**, 100 (2012).
60. A. Awasthi *et al.*, *Gran. Matter* **17**, 27 (2015).
61. A. Leonard, L. Ponson and C. Daraio, *J. Mech. Phys. Solids* **73**, 103 (2014).
62. A. Leonard, L. Ponson and C. Daraio, *Extreme Mech. Lett.* **1**, 23 (2014).
63. A. Britan *et al.*, *Int. J. Multiph. Flow* **27**, 617 (2001).
64. M. Manjunath, A. P. Awasthi and P. H. Geubelle, *Gran. Matter* **16**, 141 (2014).
65. H. A. Burgoyne *et al.*, *Procedia Eng.* **103**, 52 (2015).
66. M. Tiwari, T. R. K. Mohan and S. Sen, *Gran. Matter* **18**, 1 (2016).
67. S. Sen, T. R. K. Mohan and M. Tiwari, *KONA Powder Part. J.* **34**, 248 (2017).
68. H. A. Burgoyne and C. Daraio, *Phys. Rev. E* **89**, 032203 (2014).
69. Y. Takato, S. Sen and J. B. Lechman, *Phys. Rev. E* **83**, 033308 (2014).
70. S. Y. Wang and V. F. Nesterenko, *Phys. Rev. E* **91**, 062211 (2015).
71. F. Santibanez, R. Zuñiga and F. Melo, *Phys. Rev. E* **93**, 012908 (2016).
72. A. J. Martínez *et al.*, *Phys. Rev. E* **93**, 052224 (2016).